Biophotons as neural communication signals demonstrated by *in situ* biophoton autography

Yan Sun, Chao Wang and Jiapei Dai*

Received 7th October 2009, Accepted 8th December 2009
First published as an Advance Article on the web 21st January 2010
DOI: 10.1039/b9pp00125e

Cell to cell communication by biophotons has been demonstrated in plants, bacteria, animal neutrophil granulocytes and kidney cells. Whether such signal communication exists in neural cells is unclear. By developing a new biophoton detection method, called *in situ* biophoton autography (IBA), we have investigated biophotonic activities in rat spinal nerve roots *in vitro*. We found that different spectral light stimulation (infrared, red, yellow, blue, green and white) at one end of the spinal sensory or motor nerve roots resulted in a significant increase in the biophotonic activity at the other end. Such effects could be significantly inhibited by procaine (a regional anaesthetic for neural conduction block) or classic metabolic inhibitors, suggesting that light stimulation can generate biophotons that conduct along the neural fibers, probably as neural communication signals. The mechanism of biophotonic conduction along neural fibers may be mediated by protein–protein biophotonic interactions. This study may provide a better understanding of the fundamental mechanisms of neural communication, the functions of the nervous system, such as vision, learning and memory, as well as the mechanisms of human neurological diseases.

Introduction

Ultraweak photon emission (UPE, in short biophotons) has been found in various organisms, such as microorganisms, plants and animals, including mankind.[1–6] The change of biophotonic activity is noticeable under physiological and pathological conditions. For example, mechanical, thermal and chemical stresses, mitochondrial respiration, the cell cycle and cancer growth lead to these biophotonic activities.[7–14] In humans, there is evidence to suggest that the change of biophotonic activity is related to the consciousness, meditation, the phosphene phenomenon and conditions of acupuncture meridians,[15–18] suggesting that biophotons may play an important role in the function of the nervous system.

Cell to cell communication by biophotons has been demonstrated in plants, bacteria and certain animal cells. Early in the last century, it was shown that the induction of mitosis from the tip of an onion root could propagate to a second onion root triggered by UV light.[19] Later, the German physicist Popp and coworkers performed experiments with gonyaulax polyedra, a single-celled maritime bacterium capable of the luciferin–luciferase reaction. He placed two cuvettes containing these bacteria onto two photomultipliers and recorded the dramatic increase in synchronised photon emission upon removing the optical separation between the two vessels.[20] In 1992, a tissue culture experiment was reported where baby hamster kidney (BHK) cells were inoculated on one side of a glass film, the opposite side of which was covered with a 2–3 day old confluent layer of BHK cells. 7 h after attaching and spreading in the absence of visible light, most of the cells had aligned their long axes in the direction of the whorls of the confluent cells opposite. The effect was inhibited by a thin metal coating on the glass films. In contrast, a thin coat of silicon on the glass did not inhibit the effect, suggesting that it was caused by red or near-infrared light. The phenomenon was named "cellular vision".[21] In 1994, experiments of a similar design were performed using pig neutrophil granulocytes. Two cuvettes containing pig neutrophils were placed on two photomultiplier tubes. Bacterial extracts were placed into one cuvette, causing degranulation and light emission. Upon removal of the optical separation, light was also emitted from the other cuvette, indicating the induction of degranulation by light.[22] Based on these research data, the question is raised as to whether neural cells also have a similar mechanism to other cell populations. In this paper, we address this question by developing and using a new biophoton detection method.

Material and methods

Biophoton imaging and *in situ* biophoton autography (IBA) for germinating green bean seeds

Green bean seeds were germinated according to a previous report[23] and their skins removed before further experiments were begun. The experiments were carried out at room temperature (24 °C) unless indicated otherwise. Prepared germinating green bean seeds were placed on the specimen stage of a stereomicroscope (AZ100, Nikon, Japan) with an objective lens (AZ-Plan Apo 0.5× or 1×). Biophotons were detected and imaged using a new generation of ultra low light detector-electron multiplier CCD camera (EM-CCD; C9100-13, Hamamatsu Photonics K. K., Hamamatsu, Japan) in water cool mode (in this situation, the working temperature at the CCD can be maintained as low as −90 °C). The EM-CCD camera was mounted on top of a stereomicroscope, which was set in a completely dark box in a

Wuhan Institute for Neuroscience and Neuroengineering, South-Central University for Nationalities, Minyuan Road 708, Wuhan 430074, China. E-mail: jdai@mail.scuec.edu.cn; Fax: +86 27-67840917; Tel: +86 27-67841165

dark room. Biophotons were detected and imaged for 10 min. The other setup parameters for the EM-CCD camera during imaging were 1200× gain and 2 × 2 binning.

Light illumination was applied to the germinating green bean seeds by an LED lamp (white, 410–600 nm, 10 000–12 000 mcd) supplied by a 3 V direct current (DC) for 1 min before imaging or IBA was carried out. In addition, in order to carry out biophoton imaging and IBA at different temperatures, the germinating green bean seeds were placed on a small plate, which was placed and fixed onto a large plate with ice, 37 °C or 50 °C water.

For IBA, the germinating green bean seeds were immersed in 10% $AgNO_3$ in a container and placed in a completely dark box in dark room for 30 min. After washing with de-ionized water for 1 h and then 10% sodium thiosulfate for 10 min in the dark room, the green bean seeds were checked with a stereomicroscope and photographed using a CCD camera.

To coat the germinating green bean seeds with a neutral balsam, the seeds were quickly dried using an electric hair drier and immersed into 2% neutral balsam diluted with xylene for a few seconds. Next, before the further experiments were carried out, the seeds were completely dried in same way.

Biophoton imaging and IBA for rat brain slices, sciatic nerve and spinal nerve roots *in vitro*

The experiments were carried out on male or female adult Sprague–Dawley rats (SD, 200–300 g) purchased from the Experimental Animals Center of Tongji Medical College of Huazhong University of Science and Technology. All animal experiments were approved by the Animal Care Committee of South-Central University for Nationalities. The rats were decapitated, and their brains removed and cut into thick (300 μm) coronal slices from the anterior part of the olfactory cortex to the posterior part of the hippocampus. The 1 cm long sciatic nerve was dissected. The lumbar spinal cord, together with the attached spinal nerve roots (L1 below), were removed from the vertebra. The prepared brain slices and lumbar spinal cords were immediately placed in a container with pre-cooled (0–4 °C) modified artificial cerebrospinal fluid (M-ACSF; 252 mM sucrose, 26 mM $NaHCO_3$, 1.8 mM KH_2PO_4 and 10 mM D-glucose; pH 7.6; osmolarity 312 mOsm L^{-1}). Sucrose was substituted for NaCl to maintain a constant osmolarity and remove Cl^- from the incubation solution, which could be combined with Ag^+, producing chemical deposits.

A gas mixture of 95% O_2 and 5% CO_2 was constantly supplied *via* a membrane oxygenator placed in the M-ACSF.[24] The 1 cm long spinal motor and sensory nerve roots were dissected from the prepared lumbar spinal cords for further pre-incubation. After 1–2 h of pre-incubation and temperature equilibrium (to room temperature), the brain slices, sciatic nerve or spinal nerve roots were transferred to a cell culture dish (3.5 cm in diameter) to carry out IBA and biophoton imaging for 30 min using the EM-CCD camera, as described above. The specific steps for the IBA procedures were as follows: (1) tissues immersed in 10% $AgNO_3$ in a container for 30 min in a dark box in a dark room; (2) rinse in 252 mM sucrose for 15 min; (3) fixation by 10% formaldehyde for 5 min; (4) rinse in de-ionized water for 5 min; (5) rinse in 10% sodium thiosulfate for 15 min; (6) post-fixation by 4% polyformaldehyde in 0.1M PBS overnight; (7) immersion in 20% sucrose for 1–2 days for cryoprotection; (8) section on a cryostat (30 μm) for brain slices and sciatic nerve (not necessary for spinal nerve roots). Sections were then collected in distilled water and mounted on gelatin-coated slides, dehydrated, cleared and coverslipped. The spinal nerve roots could be directly mounted on the slides, dehydrated, cleared and coverslipped after post-fixation by 4% polyformaldehyde. In addition, in order to avoid light exposure, the experiments were undertaken in a dark room, especially steps 1 to 6, and always keeping the tissues in a dark box, except when the necessary experimental manipulations, such as solution replacement, had to be undertaken. In this situation, a weak red light could be used in the dark room.

Light stimulations and IBA in rat spinal nerve root preparations *in vitro*

Spinal motor and sensory nerve roots were prepared as described above. About 2 cm long motor and sensory nerve roots were dissected from the spinal cord and placed into the channel with one end (8 mm in length) remaining in Hole A and the other end in Hole B (Fig. 1). The part of the nerve root in Hole A was supported by a stainless wire (0.3 mm in diameter). Hole A and the channel were filled with modified cerebrospinal fluid (M-CSF) during light stimulation.

Filling the M-CSF and handing the nerve roots into the IBA effecter were undertaken in a bright room and viewed by an operating microscope. 10% $AgNO_3$ was quickly introduced into Hole B in a dark room under the guide of a weak red light, allowing about a 3 mm long nerve root to be immersed in the 10% $AgNO_3$. Light stimulations were applied for 30 min in a dark room. Next, the further experimental steps with the spinal nerve roots were carried out, as described above (steps 2–6). For the inhibitory experiments, the spinal nerve roots were pre-incubated for 1 h in a container containing 1% procaine, 50 mM 2-deoxy-D-glucose and 0.05% sodium azide or both together, diluted with M-ACSF. The spinal nerve roots were then transferred to the IBA effecter for light stimulation. As controls, the same treatments were done without light stimulation.

After IBA had finished, the spinal nerve roots were mounted onto gelatin-coated slides, dehydrated, cleared and coverslipped. The optical intensity (deposited granular sliver as IBA signals) from the segment of each nerve root immersed in 10% $AgNO_3$ during light stimulation was measured by a motorized advanced research microscope (ECLIPSE 90i, Nikon, Japan) equipped with a Nikon color cooled CCD camera (DS-5MC-U2) and controlled by Nikon image analysis software (NIS-Elements BR 3.0).

Statistical analysis

Two-tailed Student's t-tests (calculated using Microsoft Excel) or one-way ANOVA were used. All summary bar graphs are presented as mean ± s. e. m., with the significance denoted as follows: $*P < 0.05$, $**P < 0.01$.

Results

Development and evaluation of *in situ* biophoton autography (IBA)—a new method for biophoton detection at the cell level

Since with the already available photon detection methods, such as photon counting apparatus or the new generation ultra low

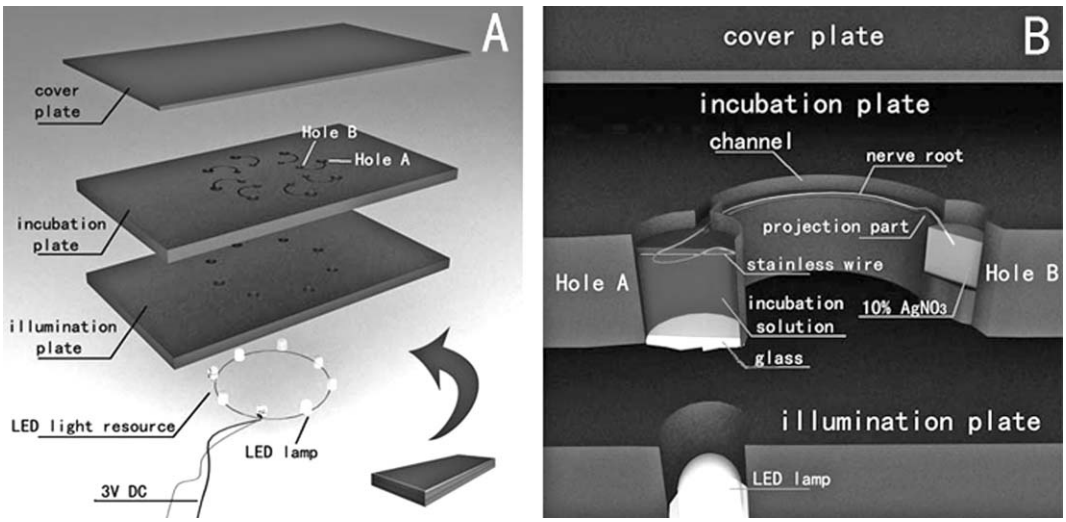

Fig. 1 Schematic drawing of the biophoton effecter. The biophoton effecter is made of an LED light resource and three black rubber plates (each 20 cm in length and 12 cm in width), including incubation, light illumination and cover plates (8 mm, 8 mm and 2 mm thick, respectively). Eight circular holes (Hole A1–8, 6 mm in diameter throughout) corresponding to eight smaller circular holes (Holes B1–8, 4 mm in diameter and 6 mm in depth, close at the bottom side) are drilled in the incubation plate (A1 and B1, A2 and B2 … A8 and B8). The distance between adjacent Holes A (such as Hole A1 and A2) is about 4 cm. A narrow bend channel (12 mm in length, 1.5 mm in width and 2 mm in depth) is made between Hole A and B. A small projection part is made close to Hole B against the liquid flow between Hole A and B *via* the channel. A thin glass sheet (cover glass) is stuck to the bottom side of each Hole A with glue. Eight circular throughout holes (6 mm in diameter) matching each Hole A are made on the light illumination plate. Different LED lamps are inserted into these holes, allowing light to pass through the glass at the bottom of Hole A and illuminate the segment of the nerve root incubated in Hole A, supported by a stainless wire. The cover plate is used to prevent the light from illuminating Hole B during light stimulation, and the bend channel is made for the same purpose. The LED lamps are supplied by a 3 V direct current (DC).

light detector-electron multiplier CCD (EM-CCD) cameras, it is difficult to observe and analyze biophotonic activity at the cell level, we have developed a new method called *in situ* biophoton autography (IBA). This method is similar to a histochemical staining technique with a key active ingredient, $AgNO_3$. The working mechanism is that of biophotonic activity (just like light exposure in photography), inducing an Ag^+ to Ag transformation due to electron transfer and consequently Ag deposits *in situ*. Deposited dark Ag granules are insoluble in water and organic solvents such as alcohol and xylene, and they can be viewed and localized morphologically under common light microscopes. The detailed protocols and procedures of IBA are referenced in the experimental procedures.

Using this new method, we successfully detected biophotonic signals (dark Ag granules) in different biological materials, including germinating green bean seeds (Fig. 2A), and the brain slices (Fig. 2B, Fig. 3A–D), sciatic nerve and spinal nerve roots of rats (Fig. 2C–E), since it has been demonstrated that such biological materials can emit biophotons[2,3,6,25] that can be detected by an EM-CCD camera in this study (Fig. 2F, G and I). As the visible Ag granules can be localized morphologically, they are particularly useful for carrying out the semi-quantitative analysis of biophotonic signals related to cell and tissue functions (see the further study below), since such a semi-quantitative analysis cannot be carried out by a EM-CCD camera at the cell level (Fig. 2F and G).

In order to evaluate the specificity and sensitivity of this new method, we carried out several experiments in the germinating green bean seeds, since this biological material not only emits biophotons, but also because the intensity of the biophotons can be manipulated by changes of temperature and light illumination (Fig. 4). We found that the density of Ag granules deposited on the surface of germinating green bean seeds is highly related to the intensity of the biophotons emitted from germinating green bean seeds (Fig. 5A–J). In addition, we found that only very weak biophotonic signals were detected by the EM-CCD camera (Fig. 2I) in the motor and sensory nerve roots *in vitro*. In contrast, IBA could result in strong staining (Fig. 2C–E), suggesting that IBA is more sensitive than the EM-CCD camera in this situation.

In order to prove that the formation of the visible Ag granules is due to a biophotonic effect and not because of other factors (such as chemical reactions, since Ag^+ can combine with several negative ions, such as Cl^-, which exists in various biological tissues and may result in chemical deposits), the germinating green bean seeds were coated in a thin transparent neutral balsam, which is used as a slide mounting medium. Such a treatment prevents direct contact between the germinating green bean seeds and $AgNO_3$ during IBA, but does not affect biophotonic emission. Consequently, we found that Ag granular deposits were also observed on the neutral balsam-coated surfaces of germinating green bean seeds in this situation, and that the density of the Ag granular deposits was related to the intensity of the biophotons manipulated by light illumination (Fig. 5H, J). This suggests that the formation of visible Ag granules is due to biophotonic effects. In addition, we used sodium thiosulfate (10%) to wash biological specimens during the standard processes of IBA, which removes any chemical deposits formed by chemical reactions between Ag^+ and other negative ions, such as Cl^-, *etc*.

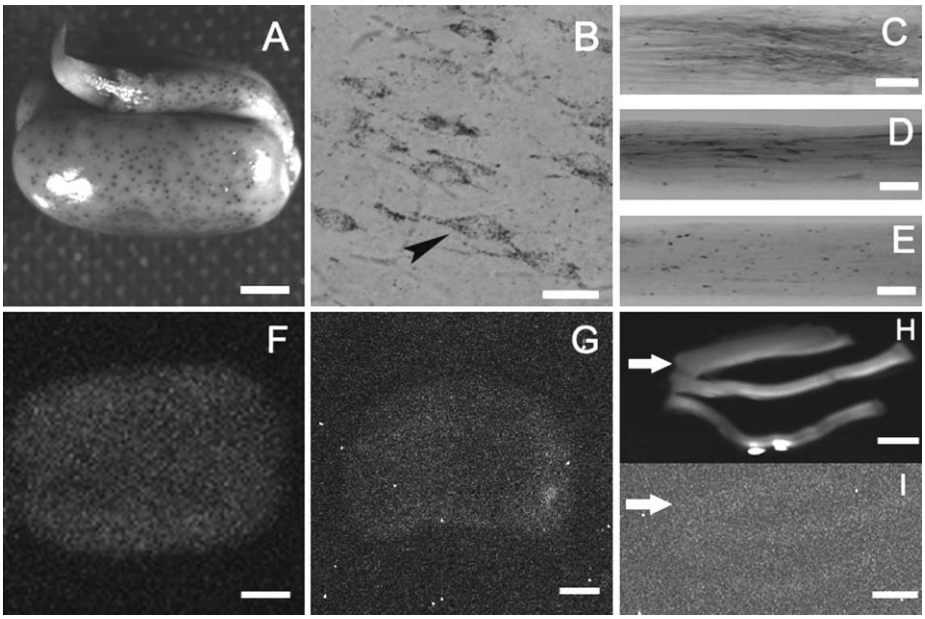

Fig. 2 Biophotons detected by the IBA method and a EM-CCD camera in different biological materials. Deposited dark granular Ag can be seen on the radical bud and cotyledons of germinating green bean seeds (**A**), cell bodies and their processes of neurons in rat striatum (**B**, arrowhead), sciatic nerve (**C**), motor (**D**) and sensory (**E**) nerve roots. Biophotonic signals detected by an EM-CCD camera from green bean seeds (**F**) and a rat brain slice (**G**). Sciatic nerve, motor and sensory nerve roots (from top to bottom in **H**, normal photography) present very weak biophotonic signals detected by an EM-CCD camera (**I**). The arrow in **H** and **I** indicates the same position. Scale bars: 1 mm for **A** and **F**; 500 μm for **C**; 300 μm for **G**, **H** and **I**; 200 μm for **D** and **E**; 25 μm for **B**.

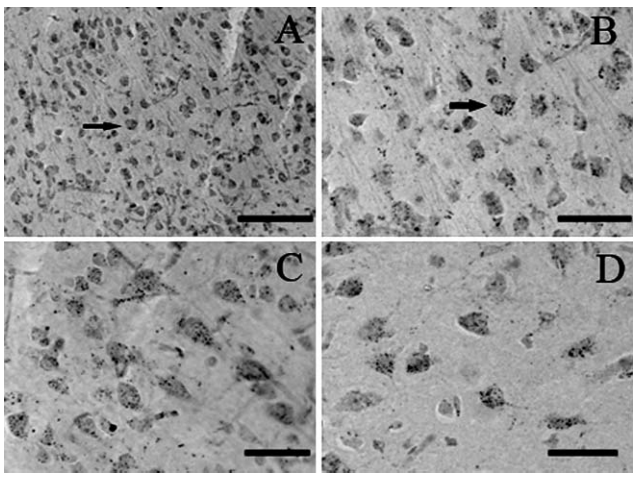

Fig. 3 Biophotonic signals in rat cortex detected by the IBA method. Deposited dark granular Ag can be seen in the various sizes of neurons in rat sensory (**A** and **B**) and motor cortex (**C** and **D**). **B** is the magnification in **A** (arrow). Scale bars: 500 μm for **A**, and 25 μm for **B**, **C** and **D**.

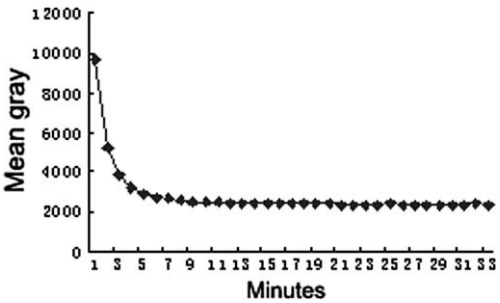

Fig. 4 The time course of attenuation of the delayed biophotonic signals after light exposure. Three germinating green bean seeds were simultaneously illuminated by a white LED light (410–600 nm, 10 000–12 000 mcd) for 1 min and immediately imaged by a EM-CCD camera for 33 min. The image each minute was continuously obtained and the mean gray of each analyzed with imaging analysis software (Simple PCI 6.0, Hamamatsu, Japan). The delayed biophotonic signals after light exposure decrease quickly and reach a baseline level within 5 min.

External light stimulation generates biophotonic activities in neural fibers

To investigate whether biophotons could serve as neural communication signals in the nervous system, we designed an instrument (Fig. 1A, B) called a biophoton effecter to observe the *in vitro* effect of external light stimulation on the biophotonic activities of the spinal motor nerve roots (MNR) and sensory nerve roots (SNR) by the IBA method. We applied various light emitting diode (LED) resources, including infrared, red, yellow, green, blue and white sources, in a dark room to illuminate the MNR or SNR incubated in M-CSF for 30 min at one end,[24] and observed the effect from the other end immersed in 10% $AgNO_3$ (for IBA). The optical density of the deposited Ag granules, representing the biophotonic signals at the segment of the spinal motor or sensory nerve roots immersed in 10% $AgNO_3$ during light stimulation, was measured by an imaging analysis system after IBA was complete. We found that the various light stimulations had a significant increase in the biophotonic activities, both in the MNRs and SNRs (Fig. 6A–C). It seems that infrared and white light is more effective for SNRs, with red and white light for MNRs, although no significant differences were found (Fig. 6A, B).

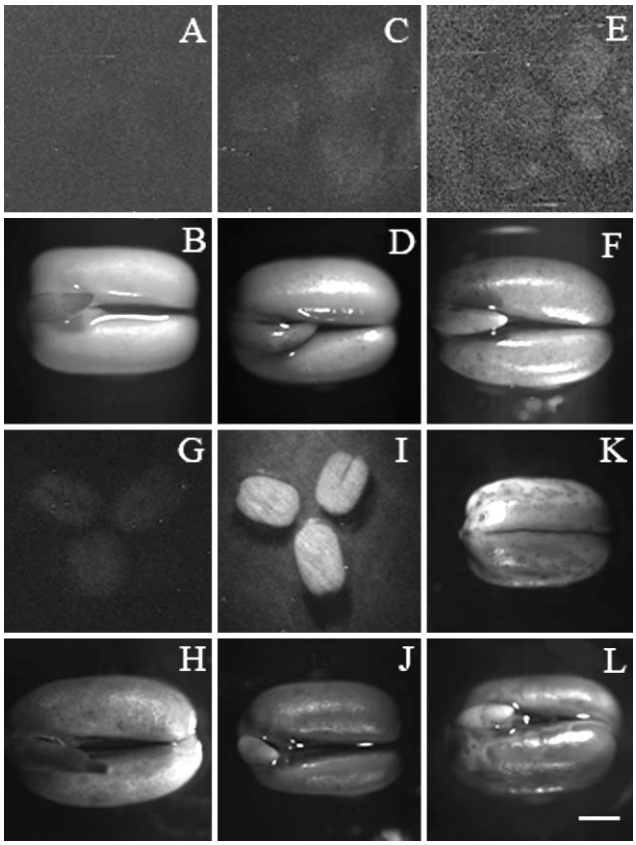

Fig. 5 The development and evaluation of *in situ* IBA with germinating green bean seeds. The intensity of biophotonic signals detected by the EM-CCD camera was temperature dependent and related to the density of the deposited dark granular Ag on the radical bud and cotyledons of the germinating green bean seeds. The zero, slight and strong biophotonic signals at 0, 37 and 50 °C, respectively (**A**, **C** and **E**) correspond to very weak, slight and strongly deposited dark granular Ag (**B**, **D** and **E**). Light exposure (white LED, 410–600 nm, 10 000–12 000 mcd) for 1 min resulted in very strong delayed biophotonic signals (**G**) and deposited dark granular Ag (**H**), as compared to controls (**I** and **J**). The germinating green bean seeds coated with a transparent thin-layer of neutral balsam still resulted in dark granular Ag deposits, which were also dependent on the light exposure. 1 min light exposure (white LED, 410–600 nm, 10 000–12 000 mcd) before IBA (**K**) *vs.* control (**L**). Scale bars: 600 mm for **A**, **C**, **E**, **G** and **I**; 300 mm for **B**, **D**, **F**, **H**, **J**, **K** and **L**.

Biophotonic conduction along neural fibers

To understand whether the observed effects are due to biophotonic conduction along the neural fibers generated by light stimulation or whether for other reasons, we studied the effects of light stimulation on the change of biophotonic activity after spinal nerve roots were treated with either a regional anaesthetic (1% procaine), a classic metabolic inhibitor (50 mM 2-deoxy-D-glucose and 0.05% sodium azide) or both for 1 h in M-CSF. Such treatments were maintained during the light stimulation period (30 min). Procaine is known to block neural conduction with little effect on oxidative metabolism.[26] The use of 2-deoxy-D-glucose and sodium azide is a classic method for metabolic inhibition.[24] We found that the significant increase of biophotonic activity by light stimulation can largely be inhibited, either by 1% procaine (Fig. 6D–F) or 50 mM 2-deoxy-D-glucose and 0.05% sodium azide (Fig. 6G, H). However, neither of them completely quenched the biophotonic activity, as compared to the control, unless both were used together (Fig. 6I). These data suggested that the observed biophotonic signals after light stimulation consist of two components: action and background biophotons.

Discussion

The present study demonstrates the development of a new method called *in situ* biophoton autography (IBA). It was successfully applied to various biological materials to detect biophotons, and it was also possible to analyze biophotonic activities in spinal nerves. This is based on the fact that biophotons (in essence, light) induce the Ag^+ to Ag transformation due to electron transfer, and consequently Ag is deposited *in situ*. In addition, the specificity and sensitivity of this new method were evaluated using the different experiments shown above, which provided experimental evidence against the doubt as to whether the observed Ag deposits really result from biophotonic signals emitted by biological materials because of the possibility of positive chemography. Therefore, the present method may contribute substantially to our understanding of biophotonic activities related to biological functions at the cell level. However, some of the limitations of this new method may need to be improved further. For example, $AgNO_3$ is corrosive and cell viability may be affected in its presence. Based on our present observations, 5% $AgNO_3$ is a suitable concentration to avoid affecting cell viability related to the biophotonic activities over certain time periods for rat brain slices and spinal nerves. In our opinion, it would be better to test for suitable concentrations of $AgNO_3$ for different biological materials. In addition, it is not known whether other alternative active ingredients, such as AgI or AgBr, could be used for this method, since these materials seem to be more sensitive to light exposure than $AgNO_3$. However, it is known that they cannot be dissolved in water to form a working solution.

We found that IBA seems to be even more sensitive than an EM-CCD camera at detecting biophotons. The fact that there is a distance between the EM-CCD camera and samples may be the main reason, since most biophoton emission is absorbed by tissue components and therefore cannot be detected externally by an EM-CCD camera. Such a shortcoming in the detection of biophotons is overcome by using the IBA method.

It is well known that $AgNO_3$ is a key component of Golgi staining, a nervous tissue staining technique discovered by Italian scientist Camillo Golgi in 1873. This technique is still widely used in modern neuroscience research more than a century later. However, to date, the mechanism by which this happens remains unclear. Thus, the use of this technique is notoriously unpredictable and the staining of neurons appears random. Based on our observations here, determining whether biophotonic emission from nervous tissue takes place could provide an explanation of the mechanism of Golgi staining and might provide new input into improving this classic technique.

In the present study, we found that biophotonic signals generated by light stimulation consist of two components: action and background biophotons. A possible explanation for this observation is that external light stimulation might generate action biophotons, being able to conduct along the neural fibers and result in an increase in biophotonic activity. Background

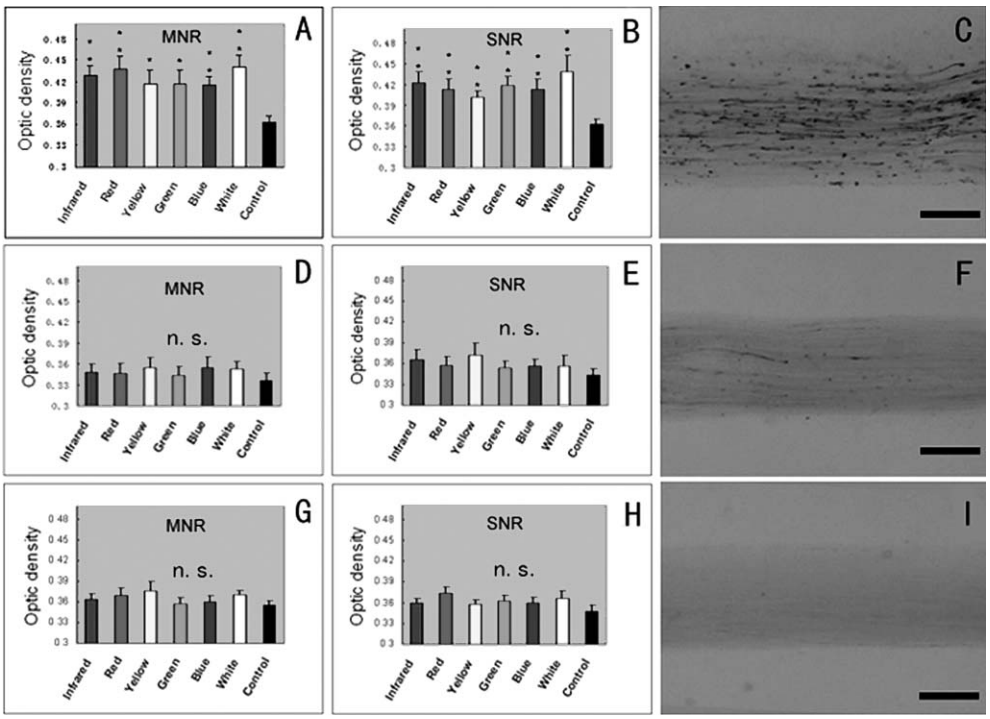

Fig. 6 The effects of light stimulation on the biophotonic activities of spinal nerve roots, and inhibitory effects by procaine and classic metabolic inhibitors. A significant increase in the biophotonic activities of MNRs and SNRs under various light stimulations, including infrared (940 nm, 2000 mw sr^{-1}), red (621–623.5 nm, 4500–5000 μcd), yellow (590–592.5 nm, 5000–6000 mcd), green (515–520 nm, 12 000–14 000 mcd), blue (460–465 nm, 4000–5000 mcd) and white (410–600 nm, 10 000–12 000 mcd) (**A**, **B**; $n = 15$ MNR and SNR from 8 animals), by comparing the optical density of IBA signals (deposited dark granular Ag) under various light stimulations with controls (without light stimulation) (two-tailed Student's t-test, asterisks indicate a significant difference $^{*}P < 0.05$ or $^{**}P < 0.01$). Strongly deposited dark granular Ag can be seen after light stimulation of an SNR (**C**). The increased biophotonic activities by light stimulation were largely inhibited by 1% procaine (**D**, **E**; $n = 11$ MNR and $n = 12$ SNR from 6 animals) or 50 mM 2-deoxy-D-glucose and 0.05% sodium azide (**G**, **H**; $n = 13$ MNR and SNR from 7 animals; n. s., $P > 0.05$; control: the same treatment without light stimulation). Weakly deposited dark granular Ag can be seen after treating with 1% procaine or 50 mM 2-deoxy-D-glucose and 0.05% sodium azide (**F**), and almost no staining by combining 1% procaine with 50 mM 2-deoxy-D-glucose and 0.05% sodium azide (**I**). The data are shown as mean ± s. e. m. Scale bars: 200 μm for **E**, **F** and **I**.

biophotons are generated *in situ*, mostly by mitochondrial oxidative metabolism due to the lipid peroxidation of mitochondrial membranes initiated by the action of the respiratory electron transport system.[11] In addition, the findings that almost no Ag granules could be observed in the spinal nerves after treating with both 1% procaine, and 50 mM 2-deoxy-D-glucose and 0.05% sodium azide, which can block neural conduction and oxidative metabolism, respectively, reinforce our explanation for the mechanism of IBA, as we discussed above, where the formation of visible Ag granules is due to a biophotonic effect, not because of other factors, such as chemical reactions.

Although we found that biophotons can be generated by external light stimulation and conducted along neural fibers, implying that biophotons might serve as neural signals, there are a few questions that still need to be answered. For example, how do biophotons conduct along neural fibers? What is the relationship between the biophotonic activity and bioelectronic activity in the nervous system? Although we have no direct experimental evidence to provide answers to these questions, a proposed mechanism called protein–protein biophotonic interactions may provide an explanation of the first point based on previous studies showing that certain proteins, such as fluorescent proteins, have unique characteristics of light absorption and emission.[27,28] In principle, as proposed in Fig. 7, two different proteins may achieve biophotonic conduction if they form a biophotonic interaction couple, meaning that one protein absorbs a certain spectral biophoton (for example 620 nm) and emits another spectral biophoton (for example

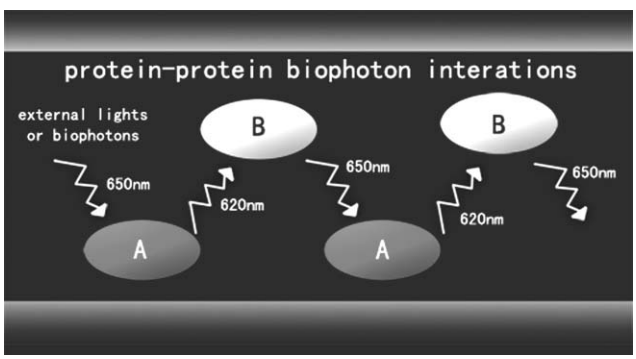

Fig. 7 A schematic drawing of protein–protein biophoton interactions for a proposed mechanism of biophoton communication. Proteins A and B are considered a biophoton interaction couple. Protein A absorbs a 620 nm biophoton and emits a 650 nm biophoton, which is absorbed by protein B. Protein B then emits a 620 nm biophoton, affecting another protein A. In such a way, biophoton communication may be achieved.

650 nm). In contrast, the other protein of the couple absorbs 650 nm biophotons and emits 620 nm biophotons. In this way, 620 and 650 nm biophotons can conduct along a neural fiber if the protein couple is distributed and assembled in a neural fiber. Similarly, different spectral biophotonic communications can be realized by different biophotonic interaction protein couples.

However, the argument might be raised that our proposal seems to contradict basic physical laws, since it is usually believed that a molecule cannot absorb low energy light and emit high energy light. However, one of the possibilities is that multi-photon excitation may emit a high energy photon if two low energy photons are simultaneously absorbed so that their energy is pooled.[29] For example, if active biophotons emitted from proteins and background biophotons generated from mitochondrial oxidative metabolism were simultaneously absorbed, then high energy photons would be generated.

It has been demonstrated that mitochondria are functionally connected and form a dynamic network within neurons.[30] Mitochondria frequently fuse and divide, and their morphology and intracellular distribution changes according to the functional demands of cells.[31] Mitochondrial networks can be electrically coupled, and can coordinate and synchronize each other.[30,32] Moreover, according to Thar and Kühl,[33] ultra-weak biophotons can be guided along a mitochondrial network and microtubules; specifically, filamentous mitochondria and microtubules may act as optical waveguides in neurons. Thus protein–protein biophotonic interactions, as well as mitochondrial interaction networks, may consist of a biophoton communication network in a neuron and its processes.

It is well accepted that the processing of information by neurons is mediated by their electrical activity, which is generated by the movement of particles, such as ions carrying electrical charges. Our finding in the present study that biophotonic activity may serve as a neural signal raises the question as to whether there is a relationship between biophotonic activity and bioelectronic activity.

Experimental data has demonstrated neural activity-dependent biophotonic activity in the brain. For example, in a previous study, the increase of biophotonic activity was found to be related to the depolarization induced by a high potassium medium, and the decrease of the biophoton activity was related to the removal of extracellular Ca^{2+} and suppressed neural activity by TTX, a voltage-dependent sodium channel inhibitor in hippocampus slices.[11] *In vivo* imaging of the spontaneous biophotonic activity in a rat's brain correlates with EEG activity.[25] In addition, pulsed electric excitation of frog sciatic nerve has been reported to cause photon emission.[34] In a recent study, it was found that focused mid-infrared light alters membrane potential and activates individual neural processes.[35] These research data suggest that biophotonic or bioelectronic activities in the nervous system are not independent biological phenomena. In our view, the interactions between bioelectronic and biophotonic activities might be an important way for neural information exchange to take place, in which bioelectronic activities may be only the basis for biophotonic activities, providing new perspectives for better understanding the functions of the nervous system, such as vision, learning and memory, as well as the mechanisms of human neurological diseases. In addition, whether biophotons could serve as fundamental signals that can carry and transfer information from one place to another in the nervous system is an interesting possibility for investigation in the future.

Conclusion

In the present study, we have demonstrated the development of a new method called *in situ* biophoton autography (IBA), which was successfully applied to various biological materials to detect biophotons. To the best of our knowledge, this is the first time biophotonic activities have been detected and analyzed using a histochemical method. Further improvements to this new method are also possible. In addition, our finding that biophotons may serve as neural communication signals could contribute substantially to understanding the biophotonic activities related to neural functions.

Acknowledgements

This work was supported by the research foundation of South-Central University for Nationalities, partly by an excellent project of the Ministry of Human Resources and Social Security of the People's Republic of China for a return overseas Chinese scholarship (2007), and the National Natural Science Foundation of China (NSFC, no. 30570629). We also thank to Dr Y. Chen for his comments on the manuscript and Liu Peng for her secretarial help.

References

1 R. P. Bajpai, P. K. Bajpai and D. Roy, Ultraweak photon emission in germinating seeds: a signal of biological order, *J. Biolumin. Chemilumin.*, 1991, **6**, 227–230.
2 Y. Isojima, T. Isoshima, K. Nagai, K. Kikuchi and H. Nakagawa, Ultraweak biochemiluminescence detected from rat hippocampal slices, *NeuroReport*, 1995, **6**, 658–660.
3 B. Devaraj, M. Usa and H. Inaba, Biophotons: ultraweak light emission from living systems, *Curr. Opin. Solid State Mater. Sci.*, 1997, **2**, 88–193.
4 R. N. Tilbury and T. I. Cluickenden, Spectral and time dependence studies of the ultraweak bioluminescence emitted by the bacterium *Escherichia coli*, *Photochem. Photobiol.*, 1988, **47**, 145–150.
5 M. Kobayashi, M. Takeda, K. I. Ito, H. Kato and H. Inaba, Two dimensional photon counting imaging and spatiotemporal characterization of ultraweak photon emission from a rat's brain *in vivo*, *J. Neurosci. Methods*, 1999, **93**, 163–168.
6 S. Cohen and F.-A. Popp, Biophoton emission of human body, *Indian J. Exp. Biol.*, 2003, **41**, 440–445.
7 R. N. Tilbury, The effect of stress factors on the spontaneous photon emission from microorganisms, *Experientia*, 1992, **48**, 1030–1041.
8 J. Slawinski, A. Ezzahir, M. Godlewski, T. Kwiecinska, Z. Rajfur, D. Sitko and D. Wierzuchowska, Stress-induced photon emission from perturbed organisms, *Experientia*, 1992, **48**, 1041–1058.
9 H. J. Niggli, Artificial sunlight irradiation induces ultraweak photon emission in human skin fibroblasts, *J. Photochem. Photobiol., B*, 1993, **18**, 281–285.
10 T. Amano, M. Kobayashi, B. Devaraj, M. Usa and H. Inaba, Ultraweak biophoton emission imaging of transplanted bladder cancer, *Urol. Res.*, 1995, **23**, 315–318.
11 Y. Kataoka, Y. Cui, A. Yamagata, M. Niigaki, T. Hirohata, N. Oishi and Y. Watanabe, Activity-dependent neural tissue oxidation emits intrinsic ultraweak photons, *Biochem. Biophys. Res. Commun.*, 2001, **285**, 1007–1011.
12 M. Nakano, Low-level chemiluminescence during lipid peroxidations and enzymatic reactions, *J. Biolumin. Chemilumin.*, 1989, **4**, 231–240.
13 Y. Z. Yoon, J. Kim, B. C. Lee, Y. U. Kim, S. K. Lee and K. S. Soh, Changes in ultraweak photon emission and heart rate variability of epinephrine-injected rats, *Gen. Physiol. Biophys.*, 2005, **24**, 147–159.

14 R.V. Wijk and E. P. Wijk, An introduction to human biophoton emission, *Forsch. Komplementarmed. Klass. Naturheilkd.*, 2005, **12**, 77–83.
15 R. Dobrin, C. Kirsch, S. Kirsch, J. Pierrakos, E. Schwartz, T. Wolff and Y. Zeira, Experimental measurements of the human energy field, in *Psychoenergetic Systems: The Interface of Consciousness, Energy and Matter*, ed. S. Krippner, Gordon and Breach, New York, 1979, 227–230.
16 T. J. Kim, Biophoton emission from fingernails and fingerprints of living human subjects, *Acupunct. Electrother. Res.*, 2002, **27**, 85–94.
17 I. Bókkon, Phosphene phenomenon: a new concept, *BioSystems*, 2008, **92**, 168–174.
18 E. P. A. Van Wijk, J. Ackerman and R. Van Wijk, Effect of meditation on hand and forehead ultraweak photon emission, *Forsch. Komplementärmed. Klass. Naturheilkd.*, 2005, **12**, 107–112.
19 A. G. Gurwitsch, The mitogenetic radiation, *Ann. Physol.*, 1934, 10.
20 F.-A. Popp, J. J. Chang, Q. Gu, and M. W. Ho, Nonsubstantial biocommunication in terms of Dicke's theory, in *Bioelectrodynamics and Biocommunication*, ed. M.-W. Ho, F.-A. Popp and U. Warnke, World Scientific Publishing, Singapore, 1994, 293–317.
21 G. Albrecht-Buehler, Rudimentary form of cellular vision, *Proc. Natl. Acad. Sci. U. S. A.*, 1992, **89**, 8288–8292.
22 X. Shen, W. Mei and X. Xu, Activation of neutrophils by a chemically separated but optically coupled neutrophil population undergoing respiratory burst, *Experientia*, 1994, **50**, 963–968.
23 C. Vidal-Valverde, New functional legume foods by germination: effect on the nutritive value of beans, lentils and peas, *Eur. Food Res. Technol.*, 2002, **215**, 472–477.
24 J. Dai, R. M. Buijs, W. Kamphorst and D. F. Swaab, Impaired axonal transport of cortical neurons in Alzheimer's disease is associated with neuropathological changes, *Brain Res.*, 2002, **948**, 138–144.
25 M. Kobayashi, M. Takeda, T. Sato, Y. Yamazaki, K. Kaneko, K. Ito, H. Kato and H. Inaba, *In vivo* imaging of spontaneous ultraweak photon emission from a rat's brain correlated with cerebral energy metabolism and oxidative stress, *Neurosci. Res.*, 1999, **34**, 103–113.
26 C. Tarba and C. A. Crăcium, Comparative study of the effects of procaine, lidocaine, tetracaine and dibucaine on the functions and ultrastructure of isolated rat liver mitochondria, *Biochim. Biophys. Acta, Bioenerg.*, 1990, **1019**, 19–28.
27 N. C. Shaner, P. A. Steinbach and R. Y. Tsien, A guide to choosing fluorescent proteins, *Nat. Methods*, 2005, **2**, 905–909.
28 X. Shu, A. Royant, M. Z. Lin, T. A. Aguilera, V. Lev-Ram, P. A. Steinbach and R. Y. Tsien, Mammalian expression of infrared fluorescent proteins engineered from a bacterial phytochrome, *Science*, 2009, **324**, 804–807.
29 R. K. Benninger, M. Hao and D. W. Piston, Multi-photon excitation imaging of dynamic processes in living cells and tissues, *Rev. Physiol., Biochem., Pharmacol.*, 2008, **160**, 71–92.
30 V. P. Skulachev, Mitochondrial filaments and clusters as intracellular power-transmitting cables, *Trends Biochem. Sci.*, 2001, **26**, 23–29.
31 M. Müller, S. L. Mironov, M. V. Ivannikov, J. Schmidt and D. W. Richter, Mitochondrial organization and motility probed by two-photon microscopy in cultured mouse brainstem neurons, *Exp. Cell. Res.*, 2005, **303**, 114–127.
32 V. N. Dedov and B. D. Roufogalis, Organisation of mitochondria in living sensory neurons, *FEBS Lett.*, 1999, **456**, 171–174.
33 R. Thar and M. Kühl, Propagation of electromagnetic radiation in mitochondria?, *J. Theor. Biol.*, 2004, **230**, 261–70.
34 V. V. Artem'ev, A. S. Goldobin and L. N. Gus'kov, Recording of light emission from a nerve, *Biophysics*, 1967, **12**, 1111–1113.
35 F. A. Wininger, J. L. Schei and D. M. Rector, Complete optical neurophysiology: toward optical stimulation and recording of neural tissue, *Appl. Opt.*, 2009, **48**, D218–D224.

